GRIFFITH UNIVERSITY

# Growth of 3C-SiC on 150-mm Si(100) substrates by alternating supply epitaxy at 1000 °C

## Author

Wang, Li, Dimitrijev, Sima, Han, Jisheng, Iacopi, Alan, Hold, Leonie, Tanner, Philip, Harrison, H Barry

## Published

2011

## Journal Title

Thin Solid Films

## DOI

10.1016/j.tsf.2011.04.224

## Rights statement

© 2011 Elsevier. This is the author-manuscript version of this paper. Reproduced in accordance with the copyright policy of the publisher. Please refer to the journal's website for access to the definitive, published version.

## Downloaded from

http://hdl.handle.net/10072/40429

## Griffith Research Online

https://research-repository.griffith.edu.au

# Growth of 3C-SiC on 150-mm Si(100) substrates by alternating supply epitaxy at 1000 °C

Li Wang, Sima Dimitrijev, Jisheng Han, Alan Iacopi, Leonie Hold, Philip Tanner,

H. Barry Harrison

Queensland Micro- and Nanotechnology Centre, Griffith University, Nathan, Queensland, 4111, Australia

*Keywords*: Silicon carbide; Low-pressure chemical vapor deposition; Alternating supply epitaxy; X-ray diffraction.

**Abstract:** To lower deposition temperature and reduce thermal mismatch induced stress, heteroepitaxial growth of single-crystalline 3C-SiC on 150 mm Si wafers was investigated at 1000 °C using alternating supply epitaxy. The growth was performed in a hot-wall low-pressure chemical vapour deposition reactor, with silane and acetylene being employed as precursors. To avoid contamination of Si substrate, the reactor was filled in with oxygen to grow silicon dioxide, and then this thin oxide layer was etched away by silane, followed by a carbonization step performed at 750 °C before the temperature was ramped up to 1000 °C to start the growth of SiC. Microstructure analyses demonstrated that single-crystalline 3C-SiC is epitaxially grown on Si substrate and the film quality is improved as thickness increases. The growth rate varied from 0.44 to 0.76 $\pm$ 0.02 nm/cycle by adjusting the supply volume of $SiH_4$ and $C_2H_2$. The thickness nonuniformity across wafer was controlled with $\pm$ 1 %. For a prime

grade 150 mm virgin Si(100) wafer, the bow increased from 2.1 to 3.1 μm after 960 nm SiC film was deposited. The SiC films are naturally *n* type conductivity as characterized by the hot-probe technique.

## 1. Introduction.

With its unique physical, chemical, electrical and mechanical properties, SiC is widely used in fabrication of next-generation electronic devices and microelectromechanical systems (MEMS) [1-4], and also potentially employed as a substrate or buffer layer in the growth of AlN, GaN and as template for the preparation of graphene layers [5-11]. Commercially available 6H-SiC and 4H-SiC wafers are small in area and very expensive compared with 3C-SiC that is the only polytype that can be heteroepitaxially grown on cheap and large-diameter Si substrates. The most commonly used method in the heteroepitaxial growth of 3C-SiC is low-pressure chemical vapour deposition (LPCVD) by simultaneous supply of Si-containing and carbon-containing sources, diluted by hydrogen ($H_2$). However, the growth of 3C-SiC using LPCVD method is usually achieved at substrate temperatures around 1350 $^{o}$C or higher [12-16], which is very close to the temperature at which Si melts and causes re-distribution of dopants in Si substrate and the accumulation of thermal mismatch stress in SiC/Si heterostructure. Great efforts have been made to reduce the deposition temperature, however, with simultaneous supply of Si-containing and carbon-containing precursors, it is reported that no single-crystalline SiC growth could be achieved below 1100 $^{o}$C [17]. As an alternative method, by utilizing alternating supply or atomic layer epitaxy method, the growth temperature was reduced to around 1000 $^{o}$C for both hetero- and homo-epitaxial growth of 3C-SiC, and the employed equipment including gas source molecular beam

epitaxy (MBE) and LPCVD reactors [17-23]. These processes enable reduction in thermal mismatch stress and wafer bowing, especially for large diameter Si substrates. With MBE reactor in use, the SiC growth was performed in the ultra high vacuum range between $10^{-4}$ and $10^{-3}$ Pa, the investigated Si-containing source was disilane ($Si_2H_6$), and the carbon-containing sources were acetylene ($C_2H_2$) and propane ($C_3H_8$) [17-21]. MBE reactors are however much more complex and expensive than LPCVD reactors, and large batch LPCVD reactors will enable commercially viable SiC deposition on large diameter Si wafers, therefore, it is preferable to achieve the growth of single-crystalline SiC on Si substrate at lower temperature in a conventional LPCVD reactor. Nagasawa *et al*. investigated the growth of SiC using dichlorosilane ($SiH_2Cl_2$) and $C_2H_2$ in a LPCVD reactor in the temperature range of 750–1050 °C [22,23]. It was found that an involvement of $H_2$ was necessary to reduce $SiH_2Cl_2$ to enable the adsorption of Si atoms on the surface of carbonized substrate [22,23]. Under intermittent flow of $H_2$, a growth of single-crystalline 3C-SiC was observed [23], however, with continuous flow of $H_2$, polycrystalline 3C-SiC was grown [23], which indicates the supply sequences of precursors and reduction gas also matters to the microstructure of grown SiC and thus makes the process complicated to control. In addition to $Si_2H_6$ and $SiH_2Cl_2$, silane ($SiH_4$) is another Si-containing precursor which is widely employed in the growth of Si and SiC crystals, and it easily decomposes at moderate temperature. Most of the articles published in open literature on the growth of SiC using alternating gas supply method focused on the study of growth kinetics and surface superstructures by low energy electron diffraction, while information on the resultant microstructural and electrical properties of grown SiC is scarcely available. In this paper, heteroepitaxial growth of single-crystalline 3C-SiC on 150 mm Si(100)

substrates by alternating supply epitaxy (ASE) using $SiH_4$ and $C_2H_2$ as precursors is demonstrated at 1000 °C using a conventional hot-wall LPCVD reactor, without the use of reduction or dilution gases. The microstructure of the grown SiC is analysed in detail. This method enables integration of 3C-SiC into mature Si device fabrication processes.

## 2. Experimental Details

Unintentionally doped 3C-SiC films of thicknesses up to 1000 nm were grown on on-axis 150 mm Si(100) substrates in a hot-wall horizontal custom made LPCVD reactor. The growth was performed at 1000 °C with $SiH_4$ (99.9994%) and $C_2H_2$ (99.9999%) as precursors. Si substrates were cleaned following the standard Radio Corporation of America (RCA) cleaning procedures prior to being loaded into the LPCVD reactor. The idle temperature of the reactor was set at 600 °C. After loading the Si wafers, the reactor temperature was ramped from 600 to 1000 °C (ramp up rate of 5 °C/min) in oxygen at a pressure of 30 Pa. The objective was to grow silicon dioxide to avoid the contamination of Si substrate by possible carbon-related residues in the reactor chamber. When reaching 1000 °C, the chamber was degassed for 30 s and $SiH_4$ (at a flow rate of 1.5 sccm (standard cubic centimeter per minute)) was introduced into the reactor for 15 min to remove silicon dioxide and then deposit a fresh Si layer on the surface of Si substrates. After that, the reactor temperature was cooled down to 750 °C in vacuum, then a flow of $C_2H_2$ (10 sccm) at the pressure of 2 Pa was introduced to convert the Si substrate surface into SiC from 750–900 °C, followed by ramping the temperature from 900 to 1000 °C with continuous flowing of $H_2$ and $C_2H_2$ at the pressure of 40 Pa (detailed gas supply procedure before epitaxial growth is shown in Fig. 1a). Then the epitaxial growth of 3C-SiC was performed cycle by cycle using ASE method, each

cycle consisted of the following four steps: 1) The supply of $SiH_4$ for 10 to 60 s with a flow rate in the range of 0.3 to 2.5 sccm; 2) Pump out for 5 to 30 s; 3) The supply of $C_2H_2$ (0.8 to 10 sccm) for 5 to 120 s; 4) Pump out for 5 to 30 s. A schematic figure describing the gas supply sequence during the epitaxial growth is shown in Fig. 1b. No $H_2$ was involved during the epitaxial growth. Microstructure analyses of epitaxial layers were performed using high-resolution x-ray diffractometry (HRXRD) and transmission electron microscopy (TEM). The $\theta$–$2\theta$ locked XRD scans were performed with CuKα radiations using a Bruker D8 advance x-ray diffraction system, the acquisions were from 30 to 95 $^{o}$ with an increment of 0.005 $^{o}$/step and a duration of each step of 0.5 s. The rocking curve scans were performed with an increment of 0.002 $^{o}$/step and a duration of each step of 0.5 s. The TEM measurements were carried out on cross-section specimens using an FEI Tecnai F30 TEM (operating at 300 kV). Film thickness was measured by a Nanometrics NanoSpec/AFT (model: 200, assuming a refractive index of 2.65) and the surface topography was observed by atomic force microscopy (AFM, model: MFP3D-BIO), the operating mode is air tapping and the radius of curvature of the cantilever tip is 10 nm. The wafer bow before and after deposition was measured by the surface profilimetry technique using Dektak 150. The conductivity type was characterized by the hot-probe technique.

Fig. 1. Schematic diagrams of the gas supply procedure: (a) before the SiC epitaxial growth and (b) during the SiC epitaxial growth.

## 3. Results and discussion

In open literature, with the initial aim of depositing one monolayer SiC per cycle on Si substrates [21,24], alternating supply epitaxy was developed, but the results showed that the growth rate varied with processing parameters [17-24]. When $Si_2H_6$ was employed as Si-containing precursor, the reported growth rate ranged from 0.28 to 1.31 nm/cycle [17-19,21,25]. Some researchers made efforts to study the dependence of growth rate on the surface superstructure of adsorbed Si atoms [17,18,24,25], however, the results were quite surprising: though the surface superstructure was found to be in (3×2) pattern, the growth rate was much higher than expected and it was suggested that excess growth rate was contributed by the physical adsorption of Si adatoms [17,18,25]. With $SiH_2Cl_2$ being as Si-containing precursor, the reported growth rate ranged from 0.12 to 1.5 nm/cycle [22,23], but it was claimed that the presence of chlorine atoms and the intermittent involvement of $H_2$ enables a self-limiting growth of SiC with a constant growth rate of 0.80 nm/cycle in a LPCVD reactor [23]. The difference in reactor pressure and the adoption of different Si-containing precursors might result in different growth mechanisms. In this study, with $SiH_4$ being employed as Si-containing precursor and without the presence of $H_2$, the growth rate varied from 0.44 to 0.76 ± 0.02 nm/cycle by adjusting the supply volume of $SiH_4$ and $C_2H_2$. For a given $SiH_4$ supply volume of 1.0 $cm^3$, the increase of $C_2H_2$ supply volume from 0.25 to 1.67 $cm^3$ resulted in the rise of growth rate from 0.57 to 0.76 nm/cycle, and correspondingly, the root mean square (RMS) roughness (in an area of 5×5 $um^2$) reduced from 25.8 to 14.6 nm (the AFM image of 400 nm SiC grown with $C_2H_2$ supply volume of 1.67 $cm^3$ is shown in Fig. 2), which demonstrated that higher carbon supply volume improves surface smoothness and increases the growth rate. The thickness across wafer was measured by

Nanospec using standard 9 points method, and thickness nonuniformity was controlled with ± 1 %.

Fig. 2. AFM image in an area of 5×5 $um^2$ for 400 nm SiC film grown with $C_2H_2$ supply volume of 1.67 $cm^3$ (RMS roughness is 14.6 nm).

The orientation and crystal quality of the grown SiC films on Si(100) substrates were characterized by XRD, all the films studied below were grown with a growth rate of 0.76 nm/cycle. For a 960 nm SiC film grown on a Si substrate (the XRD $\theta$–$2\theta$ locked scan is shown in Fig. 3, the total process time was around 24 h), besides Si(400) peak, only 3C-SiC(200) and (400) diffraction peaks were detected, indicating that single-crystalline 3C-SiC film is epitaxially grown on Si(100) substrate. The same results were also derived from SiC films with thicknesses of 225, 300, and 620 nm. The intensities of 3C-SiC(200) and (400) diffraction peaks increase with increasing film thickness. The improvement of SiC film crystal quality was revealed by the continuous reduction in full-width at half-maximum (FWHM) of 3C-SiC(200) diffraction peak (as shown in Fig. 4), decreasing from $0.30^{o}$ (225 nm epilayer) to $0.22^{o}$ (960 nm epilayer).

Fig. 3. XRD $\theta$–$2\theta$ locked scan of 960 nm SiC on Si(100) substrate.

Fig. 4. FWHM data of SiC(200) diffraction peak at various thicknesses.

To carefully examine the crystal quality, rocking curve scans of 3C-SiC(200) diffraction peak were performed and their FWHM data are shown in Fig. 5. The continuous reduction of FWHM ($0.70\,^{o}$ = 2520 arcsec for 960 nm SiC) again confirmed that crystal quality is improved with increase in film thickness. FWHM data on thin film 3C-SiC

grown on Si(100) substrate are very limited, which makes comparison difficult. For 1500 nm thick SiC grown on Si(100) substrate at 1420 $^{o}$C by simultaneous supply of $SiH_4$, $C_3H_8$, and $H_2$, the FWHM was reported in the rang of 0.67 to 0.77 $^{o}$ [14]. By altering the carbonization parameters, the FWHM of 500 nm thick SiC grown at 1350 $^{o}$C varied from 0.50 to 1.70 $^{o}$ [12]. These results indicate that the quality of the films grown at 1000 $^{o}$C is not as high as the quality of the best SiC films grown at temperatures higher than 1300 $^{o}$C. However, the quality of the SiC layer grown at 1000 $^{o}$C can be improved further by optimization of the carbonization process (as reported in Ref. 12, the quality of the carbonization layer can significantly impact the quality of the subsequently grown SiC layer).

Fig. 5. FWHM of rocking curves of 3C-SiC(200) diffraction peak at various thicknesses.

A cross-sectional TEM image of 500 nm 3C-SiC film observed along the [110] direction of electron incidence is shown in Fig. 6. It can be seen that the defect densities (comprised of stacking faults and twins) generally decreased with increasing distance from the SiC/Si interface. The selected area electron diffraction (SAED) displayed in Fig. 7 confirms that the grown 3C-SiC is single-crystal. The additional diffraction spots resulted from the presence of stacking faults in the film. The SiC/Si interface remains quite smooth and no etch pits were observed.

Fig. 6. Cross-sectional TEM image of 3C-SiC/Si observed along the [110] direction of electron incidence.

Fig. 7. SAED of 300nm 3C-SiC grown on Si(100) substrate observed along the [110] direction of electron incidence.

The wafer bow before and after deposition of 960 nm of SiC is shown in Fig. 8. Because the maximum scan length by Dektak 150 for bow measurements is 48 mm, the bow was measured at the 48-mm central region of a 150 mm wafer (scan start and end points symmetrically positioned 24 mm away from the wafer centre). The bow of the virgin prime grade 150 mm Si(100) wafer was found to be 2.1 μm, which increased to 3.1 μm after 960 nm SiC film was deposited. The measured bow after SiC deposition is insignificant in comparison to the tolerance for prime grade Si wafers which is in the order of tens of μm.

Fig. 8. Wafer bow before and after deposition of 960 nm SiC on a prime grade 150 mm Si(100) wafer.

Hot probe technique was employed to characterize the conductivity type of unintentionally doped 3C-SiC film. A negative voltage reading on the cold probe with respect to the hot probe (the hot probe was grounded) indicated that those films are of *n* type conductivity.

## 4. Conclusions

To conclude, the growth of single-crystalline 3C-SiC on 150-mm Si substrates was demonstrated at a temperature of 1000 $^{o}$C in a hot-wall LPCVD reactor using alternating supply epitaxy method, the precursors were $SiH_4$ and $C_2H_2$. It is experimentally

demonstrated that heteroepitaxial growth of 3C-SiC on Si substrates can be performed with $SiH_4$ using ASE method. Microstructure analyses conducted by XRD and TEM indicated that single-crystalline 3C-SiC is epitaxially grown on Si substrate and the continuous reduction in FWHM of rocking curve of 3C-SiC(200) diffraction peak proved that the film quality is improved as thickness increases. The growth rate varied from 0.44 to 0.76 $\pm$0.02 nm/cycle by adjusting the supply volume of $SiH_4$ and $C_2H_2$. For a given $SiH_4$ supply volume, the increase of $C_2H_2$ supply volume not only increased the growth rate but also reduced the surface RMS roughness. The thickness nonuniformity across wafer was controlled with $\pm$ 1 %. For a prime grade 150 mm virgin Si(100) wafer, the bow increased from 2.1 to 3.1 μm after 960 nm SiC film was deposited. Unintentionally doped SiC films are of *n* type conductivity as shown by hot probe measurements. All these results demonstrate that ASE is an effective method to achieve heteroepitaxial growth of single-crystalline 3C-SiC on Si substrate at a relative lower temperature of 1000 $^{o}$C using $SiH_4$ and $C_2H_2$ in a conventional LPCVD reactor.

## Acknowledgements

This work was funded by Qs Semiconductor Corporation. The authors wish to thank Dr. Kevin Jack, Ms. Anya Yago, and Prof. Jin Zou at The University of Queensland and Ms. Yu Zhao at Griffith University for their assistance in performing XRD and TEM characterization.

## References

[1] D. Nakamura, I. Gunjishima, S. Yamaguchi, T. Ito, A. Okamoto, H. Kondo, S. Onda, and K. Takatori, Nature 430 (2004) 1009.

[2] T. Lee, S. Bhunia, and M. Mehregany, Science 329 (2010) 1316.

[3] N. Moronuki, M. Kojima, and A. Kakuta, Thin Solid Films 516 (2008) 5344.

[4] D.J. Young, J. Du, C.A. Zorman, and W.H. Ko, IEEE Sens. J. 4 (2004) 464.

[5] J. Komiyama, Y. Abe, S. Suzuki, and H. Nakanishi, Appl. Phys. Lett. 88 (2006) 091901.

[6] Y.Cordier, M. Portail, S. Chenot, O. Tottereau, M. Zielinski, and T. Chassagne, J. Cryst. Growth 310 (2008) 4417.

[7] J. Komiyama, Y. Abe, S. Suzuki, H. Nakanishi, and A. Koukitu, J. Cryst. Growth 311 (2009) 2840.

[8] Y. Cui, V.K. Lazorov, M.M. Goetz, H. Liu, D.P. Robertson, M. Gajdardziska-Josifovska, and L. Li, Appl. Phys. Lett. 82 (2003) 4666.

[9] G.M. Rutter, J.N. Grain, N.P. Guisinger, T. Li, P.N. First, and J.A. Stroscio, Science, 317 (2007) 219.

[10] J.S. Moon, D. Curtis, S. Bui, T. Marshall, D. Wheeler, I. Valles, S. Kim, E. Wang, X. Weng, and M. Fanton, IEEE Electron Device Lett. 31 (2010) 1193.

[11] A. Michon, S. Vézian, A. Ouerghi, M. Zielinski, T. Chassagne, and M. Portail, Appl. Phys. Lett. 97 (2010) 171909.

[12] M. Portail, M. Zielinski. T. Chasssagne, S. Roy, and M. Nemoz, J. Appl. Phys. 105 (2009) 083505.

[13] M.A. Capano, B.C. Kim, A.R. Smith, E.P. Kvam, S. Tsoi, and A.K. Ramdas, J. Appl. Phys. 100 (2006) 083514.

[14] W. Chen, W. Wang, J. Liu, C. Chen, J. Hwang, C. Huang, and L. Chang, J. Electrochem. Soc. 157 (2010) H377.

[15] H. Nagasawa, K. Yagi, T. Kawahara, N. Hatta, and M. Abe, Microelectron. Eng. 83 (2006) 185.

[16] A. Severino, C. Bongiorno, N. Piluso, M. Italia, M. Camarda, M. Mauceri, G. Condorelli, M.A. Di Stefano, B. Cafra, A. La Magna, F. La Via, Thin Solid Films 518 (2010) S165.

[17] T. Yoshinobu, M. Nakayama, H. Shiomi, T. Fuyuki, and H. Matsunami, J. Cryst. Growth, 99 (1990) 520.

[18] T. Fuyuki, T. Yoshinobu, and H. Matsunami, Thin Solid Films 225 (1993) 225.

[19] T. Yoshinobu, H. Mitsui, Y. Tarui, T. Fuyuki, and H. Matsunami, J. Appl. Phys. 72 (1992) 2006.

[20] K. Kim, S. Choi, and K.L. Wang, Thin Solid Films, 225 (1993) 235.

[21] T. Hatayama, Y. Tarui, T. Fuyuki, and H. Matsunami, J. Cryst. Growth 150 (1995) 934.

[22] H. Nagasawa, and Y. Yamaguchi, Thin Solid Films 225 (1993) 230.

[23] H. Nagasawa, and K. Yagi, Phys. Status Solidi B 202 (1997) 335.

[24] S. Hara, T. Meguro, Y. Aoyagi, M. Kawai, S. Misawa, E. Sakuma, and S. Yoshida, Thin Solid Films 225 (1993) 240.

[25] T. Fuyuki, M. Nakayama, T. Yoshinobu, H. Shiomi, and H. Matsunami, J. Cryst. Growth, 95 (1989) 461.

## Figure captions

Fig. 1. Schematic diagrams of the gas supply procedure: (a) before the SiC epitaxial growth and (b) during the SiC epitaxial growth.

Fig. 2. AFM image in an area of 5×5 $um^2$ for 400 nm SiC film grown with $C_2H_2$ supply volume of 1.67 $cm^3$ (RMS roughness is 14.6 nm).

Fig. 3. XRD $\theta$–$2\theta$ locked scan of 960 nm SiC on Si(100) substrate.

Fig. 4. FWHM data of SiC(200) diffraction peak at various thicknesses.

Fig. 5. FWHM of rocking curves of 3C-SiC(200) diffraction peak at various thicknesses.

Fig. 6. Cross-sectional TEM image of 3C-SiC/Si observed along the [110] direction of electron incidence.

Fig. 7. SAED of 300nm 3C-SiC grown on Si(100) substrate observed along the [110] direction of electron incidence.

Fig. 8. Wafer bow before and after deposition of 960 nm SiC on a prime grade 150 mm Si(100) wafer.

Figures

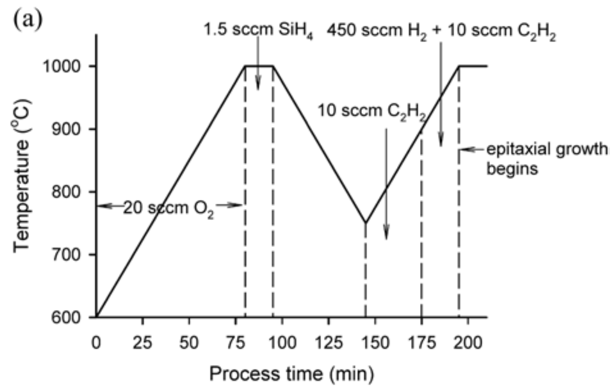


Fig. 1(a)

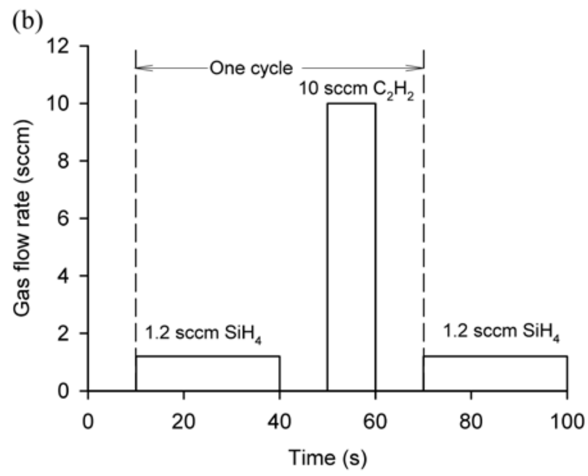


Fig. 1(b)

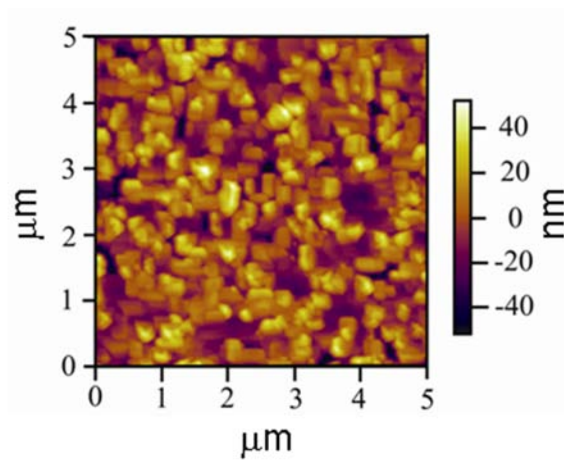


Fig. 2

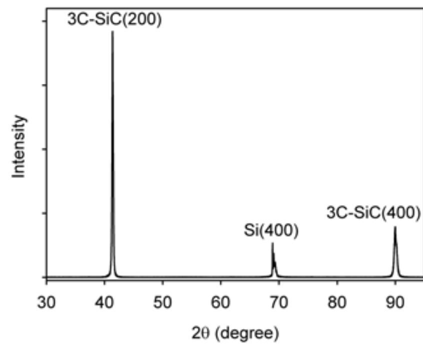

Fig. 3

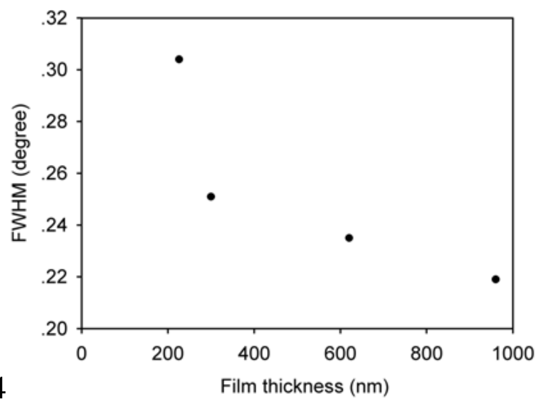

Fig.4

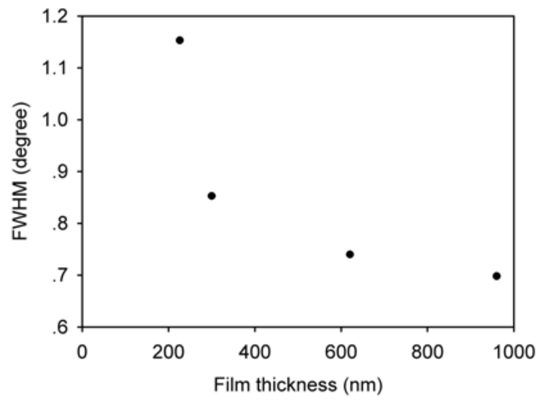

Fig. 5

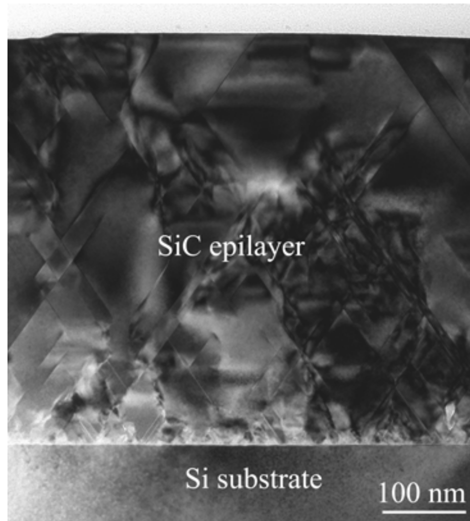

Fig. 6

Fig. 7

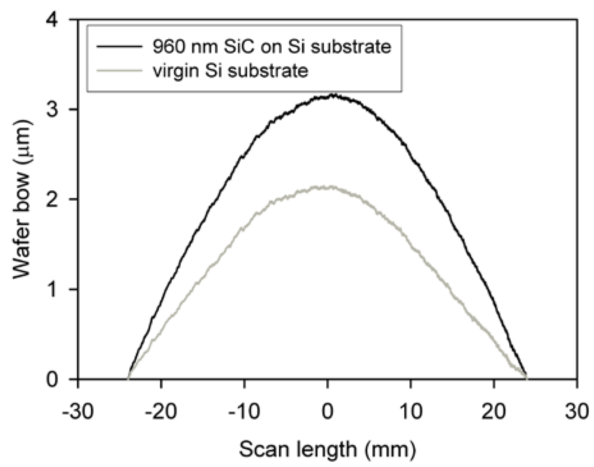

Fig. 8